Indonesian Journal of Electrical Engineering and Informatics (IJEEI)
Vol. 9, No. 3, September 2021, pp. 633~646
ISSN: 2089-3272, DOI: 10.52549/ijeei.v9i3.2892

Modeling and Fabrication of Smart Robotic Wheelchair Instructed by Head Gesture

Muhammad Mudassir[1], Anas Mujahid[2]
[1]Department of Electronics Engineering, Hamdard University, Karachi, Pakistan.
[2]Key Laboratory for Physical Electronics and Devices of the Ministry of Education & Shaanxi Key Lab of Information Photonic Technique, Xi'an Jiaotong University, Xi'an 710049, China.

Article Info

Article history:

Received Nov 29, 2020
Revised May 30, 2021
Accepted Jul 15, 2021

Keywords:

Quadriplegic
Accelerometer
Wireless communication
ATmega328 controller
Gyroscope
Power MOSFETs
DC geared motors

ABSTRACT

The confronting problem faced by the handicapped, paralyzed, disabled, and quadriplegic people is their independent mobility. They need external assistance to perform their daily life activities. This paper aims to solve that problem by smart designing and deployment of the robotic wheelchair for those who cannot perform their voluntary activities and movements. The proposed automated wheelchair comprises two parts; the first part is the user's helmet that works as a master device, and the second part is a slave device, a smart wheelchair. The master device consists of an accelerometer, microcontroller, and wireless transmitter, in which the Accelerometer recognizes the movements of the user's head and transmits the signal according to the tiltation of the user's head. Besides this, the slave device consists of a wireless receiver, microcontroller, Gyroscope, power MOSFETs, and DC geared motors mounted on a smart wheelchair, which response as per the instructions of the master device. Furthermore, the paper also provides a brief construction of this mechatronic and amphibian system using static and dynamic equations.

Corresponding Author:

Muhammad Mudassir,
Department of Electronics Engineering,
Hamdard University,
Madinat al-Hikmah, Hakim Mohammad Said Road, Karachi – 74600, Pakistan.
Email: mudassirusman.mu@gmail.com

1. INTRODUCTION

Mobility and self-dependency are essential for a good quality of daily life. Loss of mobility due to an accident, injury, or illness is usually accompanied by a loss of a comfortable life and that person dependent on others. The paralyzed, handicapped, and disabled diseases usually include quadriplegic and paraplegic persons. People with quadriplegia are persons who cannot move their four limbs except the head, where paraplegics are persons who cannot move their two limbs.

The cause for such an increase in mobility impairment, as shown in Figure 1, can be different: arthritis, stroke, high blood pressure, degenerative diseases of joints & bones, cases of paralysis, and congenital disabilities. Also, quadriplegia appears because of accidents or age [2]. There have been several tests to overcome this problem, such as walking aid robots, muscle suit for nursing care, electric wheelchair, and electrical nursing robots. They commonly use an electric wheelchair because it can support older people who, by their hand-power, have trouble driving a wheelchair and typically don't need much support from care staff. Therefore, for a long time, the electric wheelchair was invented. There are, however, several issues with the electric wheelchair [3]. There are a variety of methods and techniques have been proposed in the world. For example, Shayban Nasif et al. [4] have used a Head gesture recognition acceleration sensor and RF module (radio frequency) for wireless control. Umar Mohammad et al. [5] proposed a MATLAB script, and the webcam performs retina capture. Recently, Brain-Computer Interface (BCI) techniques have also been widely

used to assist human problems, more specifically to assist paralyzed people [6]. Various BCI techniques using eye blinks, EEG signals have been deployed to volunteer quadriplegic persons [7-9].

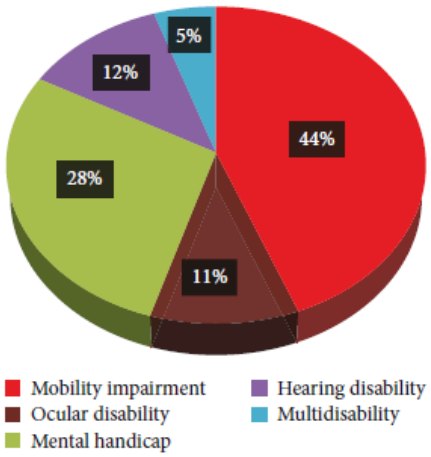

Figure 1. The distribution of handicap prevalence in Tunisia in 2013 [1]

Eye motion is detected, and the motion tracking system begins to track the chair's movement through the webcam and ATmega1284P virtual serial communication. Steering control two-wheeled wheelchair designed has also been adopted, which has no caster and moves with only two wheels [10]. The gyro sensor measures the body's pitch angle, and the two in-wheel motors are used for moving the body. Rini Akmeliawati et al. [11] designed the wheelchair system, which regulates its movement by merely bending the fingers of a person. In order to control the wheelchair, a type of sensor known as 'flex-sensors' is incorporated into a hand glove. Nowadays, the tongue-controlled wheelchair has also become a famous technique [12], but this technique requires embedding sensors on the tongue, leading to serious problems if the sensor slips into the mouth or is ingested. Md Ashiqur Rahman Apu et al. [13] proposed a wheelchair that is used to detect intentional eye blinks by processing eyeball images of the subject. An algorithm is suggested to generate a command of wheelchair movement from consecutive intentional eye blinks. Image processing techniques are implemented using raspberry-pi to detect deliberate eye blinks from eyeball images. The authors' systems we discussed above are controlled by retina capture, steering control (caster-less), intentional eye blink, and finger bending techniques; moreover, the RF Modules is used for wireless communication. To addresses the problems found in the wheelchairs built above, a robotic wheelchair is developed based on MEMS technology; an accelerometer is used instead of the above techniques in which we can vary and set the particular range or angle of head tiltation as per the requirement when the head tilts and cross that particular range or angle, the wheelchair will start moving in the desired direction [14]. It is speechless the issues present in eye-controlled wheelchairs such as dim environment control, eyes strain, and very low precision & accuracy [15]. It also eliminates the un-stability & inefficiency in the steering control (caster-less) system and a very much cost-effective & appropriate technique compared to the fingers bending method. Controlling any actuator or wheelchair with the help of an Accelerometer is more reliable and user-friendly way than the above authors' approach. Our proposed system is wireless; there is no wired connection between the head circuit and wheelchair circuit. In our wheelchair, Bluetooth in the master-slave combination is used for wireless communication between data, which has no high-power consumption, antenna, and interference issues, unlike the RF module [16]. Moreover, the gyroscope has been used in a developed system, which helps to maintain the speed and excellent stability of a wheelchair on concrete or rough surfaces and on an inclined plane. Furthermore, highly torque DC geared motors are used in a designed system for smooth performance and efficient power transmission.

2. MODEL AND DESIGN

2.1. Mathematical modeling of the system

The wheelchair's mathematical model is built on its mechanics and kinematic equations. The geometry of the wheelchair depends on the plane's physical construction see Figure 2, while its motion in space is defined by kinematic equations [17].

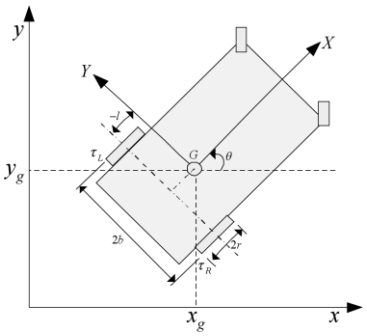

Figure 2. The platform of the wheelchair on a leveled plane

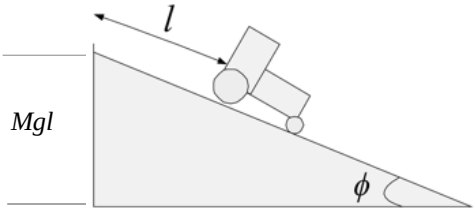

Figure 3. The platform of the wheelchair on a slope

Differential equations describing the time displacement of the wheelchair, but taking into account the kinematic constraints, were derived using Lagrange formalism see Equation 1 [17].

$$L = \frac{1}{2}M(\dot{x}_g^2 + \dot{y}_g^2 + \dot{z}_g^2) + \frac{1}{2}I_Z\dot{\theta} + lM\dot{\theta}\cos\phi(\dot{x}_g\sin\theta - \dot{y}_g\cos\theta) - Mg\sin\phi(\dot{x}_g\cos\theta + \dot{y}_g\sin\theta) \quad (1)$$

The Lagrange function is represented in the following form, taking into account the position of the wheelchair in the 3D space (xyz -coordinate system) indicated by $q = (x_g, y_g, z_g, \theta)^T$ with (x_g, y_g, z_g) being the Cartesian coordinate of the wheelchair's center of gravity and θ being the angle of rotation of the wheelchair [18].

$$M(q)\ddot{q} + C(q,\dot{q})\dot{q} + G(q) = E(q)\tau + A^T(q)\lambda \quad (2)$$

Where

$$M(q) = \begin{Bmatrix} M & 0 & 0 & lMcos\phi sin\theta \\ 0 & M & 0 & -lMcos\phi cos\theta \\ 0 & 0 & M & 0 \\ lMcos\phi sin\theta & -lMcos\phi cos\theta & 0 & I_Z \end{Bmatrix}$$

$$C(q,\dot{q}) = \begin{Bmatrix} 0 & 0 & 0 & \dot{\theta}lMcos\phi cos\theta \\ 0 & 0 & 0 & \dot{\theta}lMcos\phi sin\theta \\ 0 & 0 & 0 & 0 \\ 0 & 0 & 0 & 0 \end{Bmatrix},$$

$$G(q) = \begin{Bmatrix} Mgsin\phi cos\theta \\ Mgsin\phi sin\theta \\ 0 \\ Mgsin\phi(y_g cos\theta - x_g sin\theta) \end{Bmatrix}$$

$$E(q)_{4\times 2} = \begin{Bmatrix} \frac{cos\theta}{r} & \frac{cos\theta}{r} \\ \frac{sin\theta}{r} & \frac{sin\theta}{r} \\ 0 & 0 \\ \frac{b}{r} & \frac{-b}{r} \end{Bmatrix}, \tau = \begin{Bmatrix} \tau_R \\ \tau_L \end{Bmatrix},$$

$$A(q)_{2\times4} = \begin{Bmatrix} -cos\phi sin\theta & cos\phi cos\theta & sin\phi & -l \\ sin\phi sin\theta & -sin\phi cos\theta & cos\phi & 0 \end{Bmatrix}$$

The Lagrange multiplier vector and λ. τ_L and τ_R respectively represent the left and right torque. While all are identical, in the opposite case, a rectilinear movement occurs, and rotational motion.

If lateral motions are not possible for wheelchair wheels without slipping, the matrix associated with the constraints is then written in equation form as $A = (q)\dot{q} = 0$ perpendicular to the axis of the driving wheels. Considering $S(q) \in \mathbb{R}^{n\times m}$, we derive the kinetic equation as follows: a set of smooth and linearly independent vector fields spanning the null space of $A(q)$ such that $S^T(q)A^T(q) = 0$.

$$\dot{q} = S(q)\eta \tag{3}$$

With $S(q) = \begin{Bmatrix} cos\theta & -lcos\phi sin\theta \\ sin\theta & lcos\phi cos\phi \\ 0 & lsin\phi \\ 0 & 1 \end{Bmatrix} and\ \eta = \begin{pmatrix} \upsilon \\ \omega \end{pmatrix}$

The speeds υ and ω are the linear and angular velocities of the distinguished point G, the wheelchair center of gravity, and the user combined, respectively.

With relation to time, the derivative of Equation 2 gives

$$\ddot{q} = \dot{S}(q)\eta + S(q)\dot{\eta} \tag{4}$$

With the matrix $\dot{S}(q) = \begin{Bmatrix} -\dot{\theta}sin\theta & -\dot{\theta}lcos\phi cos\theta \\ \dot{\theta}cos\theta & -\dot{\theta}lcos\phi sin\theta \\ 0 & 0 \\ 0 & 0 \end{Bmatrix}$

Taking Equation 3 and 4 into Equation 2 and simplifying it, we obtain a more fitting representation of the control system for the dynamic wheelchair model as follows.

$$\begin{Bmatrix} \dot{\upsilon} \\ \dot{\omega} \end{Bmatrix} = \begin{Bmatrix} -gsin\theta \\ \frac{Mgsin\phi(y_g cos\theta - x_g sin\theta)}{Ml^2 cos2\phi - I_Z} \end{Bmatrix} + \begin{Bmatrix} \frac{1}{Mr} & \frac{1}{Mr} \\ \frac{b}{r(I_Z - Ml^2 cos2\phi)} & -\frac{b}{r(I_Z - Ml^2 cos2\phi)} \end{Bmatrix} \begin{pmatrix} \tau_R \\ \tau_L \end{pmatrix}$$

(5)

As mentioned above, the model shows the wheelchair's reaction to a sloping flat surface. It can also be verified by the results found in [17], hence the need for a controller.

2.2. Stabilizing of the system

In order to control processes, several methods have been used. Two approaches to wheelchair regulation were applied by Dabo, and positive results were obtained for both methods. They are NCGPC and feedback linearization (Nonlinear Continuous-time Generalized Predictive Control). In this article, the latter, also implemented in [18], is used. The purpose is that the motion along the trajectory should conform to a given command.

The dynamic wheelchair model can be rewritten as a nonlinear square-MIMO structure in the following form [19].

$$\begin{cases} \dot{x} = f(x) + \sum_{j-1}^{2} g_j(x)u_j \\ y = [h_1(x), h_2(x)]^T \end{cases}$$

where $x \in \mathbb{R}^2$, $u \in \mathbb{R}^2$ and $y \in \mathbb{R}^2$ which represents the state, control input, and output vectors, respectively. The tracking error is then expressed as a tracking error as the objective is to track the trajectory from a given pair of the linear reference velocity υ_r and angular location of the wheelchair θ_r.

$$\begin{cases} e_1^1 = \upsilon - \upsilon_r \\ e_1^2 = \theta - \theta_r{}' \end{cases} \tag{6}$$

This is accomplished by linearization of input-output. If a function has a relative degree vector $\rho = (\rho_1, \rho_2)$ obtained from the successful derivation of Equation 6 concerning the time before the control input $(u_1, u_2)^T$ occurs, the input-output is linearizable in field $E \in \mathbb{R}^2$. Therefore, after applying Equation 6's Lie derivative, we have

$$\begin{cases} \dot{e}_1^1 = \dot{\upsilon} - \dot{\upsilon}_r = L_f e_1^1 + (L_{g_1} e_1^1 \quad L_{g_2} e_1^1) \begin{pmatrix} u_1 \\ u_2 \end{pmatrix} \\ \dot{e}_1^2 = \dot{\theta} - \dot{\theta}_r = \omega - \omega_r = e_2^2 \\ \dot{e}_2^2 = \dot{\omega} - \dot{\omega}_r = L_f^2 e_1^2 + (L_f L_{g_1} e_1^2 \quad L_f L_{g_2} e_1^2) \begin{pmatrix} u_1 \\ u_2 \end{pmatrix} \end{cases}$$

where

$$\begin{cases} L_{g_1} e_1^1 = -g \sin\phi \\ L_f^2 e_1^2 = \dfrac{Mg \sin\phi (y_g \cos\theta - x_g \sin\theta)}{Ml^2 \cos 2\phi - I_Z} - \dot{\omega}_r \end{cases}$$

With a relative degree vector equal to $\rho = (1, 2)$ and the decoupling matrix.

$$D(x) = \begin{Bmatrix} L_{g_1} e_1^1 & L_{g_2} e_1^1 \\ L_f L_{g_1} e_1^2 & L_f L_{g_2} e_1^2 \end{Bmatrix} = \begin{Bmatrix} \frac{1}{Mr} & \frac{1}{Mr} \\ \frac{b}{r(I_Z - Ml^2 cos2\phi)} & - \quad \frac{b}{r(I_Z - Ml^2 cos2\phi)} \end{Bmatrix} \tag{7}$$

It is then easy to rewrite Equation 3 as follows, since the number of the relative degrees $(\rho_1 + \rho_2)$ is equal to 3 more significant than the wheelchair method defined in Equation 5.

$$\begin{Bmatrix} \dot{\upsilon} \\ \dot{\omega} \\ \dot{\theta} \end{Bmatrix} = \begin{Bmatrix} -gsin\theta \\ \frac{Mgsin\phi(y_g cos\theta - x_g sin\theta)}{Ml^2 cos2\phi - I_Z} \\ \omega \end{Bmatrix} + \begin{Bmatrix} \frac{1}{Mr} & \frac{1}{Mr} \\ \frac{b}{r(I_Z - Ml^2 cos2\phi)} & - \quad \frac{b}{r(I_Z - Ml^2 cos2\phi)} \\ 0 & 0 \end{Bmatrix} \begin{pmatrix} \tau_R \\ \tau_L \end{pmatrix} \tag{8}$$

where

$$f(x) = \begin{Bmatrix} -gsin\theta \\ \frac{Mgsin\phi(y_g cos\theta - x_g sin\theta)}{Ml^2 cos2\phi - I_Z} \\ \omega \end{Bmatrix},$$

$$g_1(x) = \begin{Bmatrix} \frac{1}{Mr} \\ \frac{b}{r(I_Z - Ml^2 cos2\phi)} \\ 0 \end{Bmatrix},$$

$$g_2(x) = \begin{Bmatrix} \frac{1}{Mr} \\ -\frac{b}{r(I_Z - Ml^2 cos2\phi)} \\ 0 \end{Bmatrix}, with\ x = (\upsilon, \omega, \theta)^T.$$

It is imperative to select the state feedback law as it compensates for the nonlinearity that happens in the wheelchair's input-output behavior. For its determinant not equal to zero for $I_Z - Ml^2 \cos 2\phi \neq 0$, the decoupling matrix (Equation 7) being invertible, the state feedback law linearizing wheelchair system is provided by

$$\begin{Bmatrix} u_1 \\ u_2 \end{Bmatrix} = \begin{Bmatrix} L_{g_1} e_1^1 & L_{g_2} e_1^1 \\ L_f L_{g_1} e_1^2 & L_f L_{g_2} e_1^2 \end{Bmatrix}^{-1} \begin{Bmatrix} \upsilon_1 - L_f e_1^1 \\ \upsilon_2 - L_f^2 e_1^2 \end{Bmatrix},$$

where $\upsilon = (\upsilon_1, \upsilon_2)^T$ which is proportional to the tracking error; $\upsilon_1 = -K_1 e_1^1$ and $\upsilon_2 = -K_{21} e_1^2 - K_{22} e_2^2$. The gain matrix must be chosen such that the linearized system is stable [20].

2.3. Designing of the system

2.3.1. Terminologies used

m = Mass (kg)
r = Radius of motor shaft (m)
R = Radius of wheel (m)

a = Acceleration (m/s2)
g = Acceleration due to gravity (m/s2)
W = Weight (N)
N = Normal force (N)
f = Friction force (N)
μS = Static coefficient of friction
μD = Dynamic coefficient of friction
η = Efficiency of motor
FDRIVE = Drive force (N)
FDRIVE' = Efficient drive force (N)
υ = Velocity (m/s)
ΔF = Force due to acceleration (N)
ω = Angular speed (rad/sec)
τOPP = Opposing Torque (N.m)
τDRIVE = Drive Torque (N.m)
P = Power (W)
V = Voltage (V)
I = Current (A)

2.3.2. Payload estimation

Mechanical Structure = 33 kg
2 × Batteries = 9 kg
2 × Motors = 8 kg
Person = 85 kg
Another Stuff = 1 kg
Total Payload = 136 kg

2.3.3. Values of the variables

The radius of Motor Shaft = 6 mm
The radius of Wheel Shaft = 8 mm
The radius of Bearing Spindle Shaft = 10 mm
The radius of Wheel = 0.1397 m
The radius of Bearing Bush = 30 mm
Sprocket Ratio = 1:1
Bearing Bore Diameter = 20 mm
Bearing Diameter = 37 mm
Bearing Thickness = 9 mm
Mass = 136 kg
a = 0.01 m/s^2 for static || 0.5 m/s^2 for dynamic
g = 9.81 m/s^2
$\mu_S = 0.8$
$\mu_D = 0.4$
η = 90%

2.3.4. Speed calculations

Desired Speed (υ) = 0.190 m/s
$\upsilon = R\,\omega$
$\omega = \upsilon/R$
ω = 1.36 rad/sec
$rpm = (60\times\omega)/2\pi$
rpm = 12.9

2.3.5. Torque calculations

The overall weight is distributed between all the four tires, that is, 34 kg each. Since the wheelchair is Rear Wheel Drive (RWD), the rear wheels are responsible for accelerating the forward tires as well. Now, the weight is distributed between two tires, that is 68 kg each.

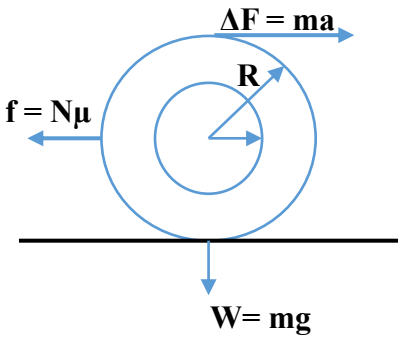

Figure 4. Physical quantities are concerned with the tire

Now, calculating the forces on each tire
Weight
W = mg
W = 667.08 N
Static calculations
Friction
N = W
f = NμS
f = 533.664 N
Opposing torque
τOPP = f×R
τOPP = 74.55 N.m
At rest, τOPP = τDRIVE
Drive force
Therefore, FDRIVE = τOPP / r
FDRIVE = 12425.47 N
At rest, we add a force equivalent to accelerate the object at a rate of 0.01 m/s2, that is; ΔF = ma
Force due to acceleration
ΔF = 0.68 N
Drive torque
τDRIVE = (FDRIVE + ΔF) × (100/η) × r (9)
τDRIVE = 82.84 N.m

Dynamic calculations
Friction
N = W
f = NμD
f = 266.832 N
Opposing torque
τOPP = f×R
τOPP = 37.27 N.m
At rest, τOPP = τDRIVE
Drive force
Therefore, FDRIVE = τOPP / r
FDRIVE = 6212.73 N
To add an acceleration of 0.5 m/s2, we add a force; ΔF = ma
Force due to acceleration
ΔF = 34 N
Drive torque
τDRIVE = (FDRIVE + ΔF) × (100/η) × r (10)
τDRIVE = 41.64 N.m
Now, calculating the total mechanical power required
Mechanical power
P = τDRIVE × ω
P = 56.63 kW

2.4. Mechanical structure

The design of the mechanical structure is entirely developed on behalf of mathematical modeling, see Equation 8, calculations and considering the effects of physical quantities. The material we have used in the mechanical structure is mild steel and a complete wheelchair structure of proper dimensions made with the help of welding and lathe machines. We have attached 2 caster wheels below the front part of the wheelchair, due to which the wheelchair can move in every direction smoothly, and the 2 rear wheels are the driving wheels, which are attached with the motor shaft with the help of a chain and sprocket. We have set the sprocket ratio 1:1 to drive the rear wheels, and this is done to reduce the mechanical load on the motor's shaft. We have used bearing in the bushes of the spindle shaft, which ensures the fluent movement of the wheelchair on every surface. The square-shaped slots are designed for mounting the motors and batteries. The structure utilizes Allen key bolts and grip screws for any joint or attachment instead of using ordinary nuts or bolts.

3. BATTERY REPORTING

3.1. Battery sizing

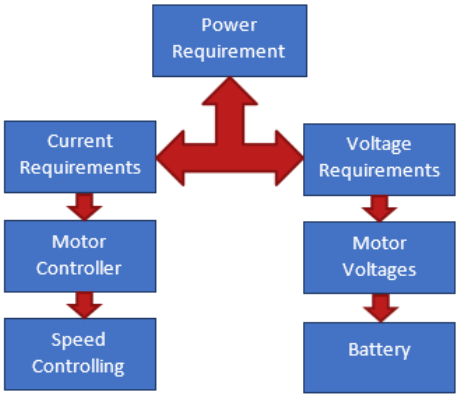

Figure 5. Battery sizing criteria

Analysis of battery sizing is used to choose the most suitable battery bank, check the full capacity of the current batteries, and easily simulate a wide range of backup, power, and other scenarios. For a given duty cycle, the Battery Sizing module specifies the number of strings, number of cells, and cell size of a battery and also compensates for real-life factors such as temperatures, aging, and initial power that relate to critical electrical systems of this kind. In order to meet the maximum system voltage during the battery charging period and the minimum system voltage during the battery discharging period, the number of cells is determined. As revealed in Figure 5, the number of strings and cell size are calculated to provide adequate load power, taking into account the minimum device voltage and the minimum operating current.

3.2. Battery selection

The power of the battery is measured in milliamps x hours (mAH). For example, if a battery has a capacity of 250 mAH and provides a load with an average current of 2 mA, the battery would theoretically last 125 hours. Nevertheless, in fact, the way the battery is discharged has an effect on the actual battery life. Typically, discharging a battery at the manufacturer-recommended rate allows the battery to deliver near its nominal power. But it is not possible to actually extrapolate the result linearly to other discharge profiles. In Table 1, we considered significant parameters for the selection of an appropriate battery. Based on consuming current, I(Amp) by the motors and desired operating timing of the system, we can select the suitable battery for our wheelchair by just calculating the battery AH capacity and voltages V(Volts).

Table 1. Parameters required for battery selection

V(Volts)	12V	24 V	36V	48V	60V
I (Amp)	5.64	2.82	1.88	1.41	1.128
Time 7 AH	1.24	2.48	3.72	4.96	6.20
12 AH	2.12	4.25	6.38	8.51	10.6

$P = V \times I$
$I = P/V$
$c = I/t$
$t = c \times I$
P = Electrical power
V = Voltage
I = Current
c = Battery capacity
t = Time

4. SOFTWARE FORMATION

The flowchart of the wheelchair acknowledged in Figure 6 revealed the software deployment of the system. We used some special libraries and functions in the software to make the hardware compatible with the software. In the programming of the master device, we also have defined and set the particular range or angle of head tiltation by using user-defined commands when the head tilts and crosses that particular range or angle, some specific alphabets generated according to the head's movement on which the operating directions of the wheelchair depend. The generated alphabets are transmitted wirelessly to the slave device. In the slave device, we used the negative axis of pitch coordinate to monitor the wheelchair's orientation continuously. Therefore, the slave device checked the angle of pitch coordinate of the wheelchair, and if the pitch angle is less than -5, this means the wheelchair is on the inclined plane, or rough surface, so different duty cycles are generated based on angles which slow down the speed of the system so that the wheelchair can move smoothly and firmly on the inclined plane. If the pitch coordinate angle is more significant than -5, this means the wheelchair is on the regular or flat surface so that the duty cycle remains 100% and no pulse width modulation generated, and the wheelchair remains at its full speed. If the head tilts on the front side, the alphabet 'f' is generated, and the wheelchair moves in the forward direction. When the head tilts on the backside, the alphabet 'b' is generated, and the wheelchair moves in the backward direction. The alphabet 'r' is generated, and the wheelchair moves in the right direction when the head tilts on the right side, and the head tilts on the left side, alphabet 'l' is generated, and the wheelchair moves in the left direction. Moreover, the wheelchair remains in a steady state when the head does not tilt on any side and remains in the center in its normal position.

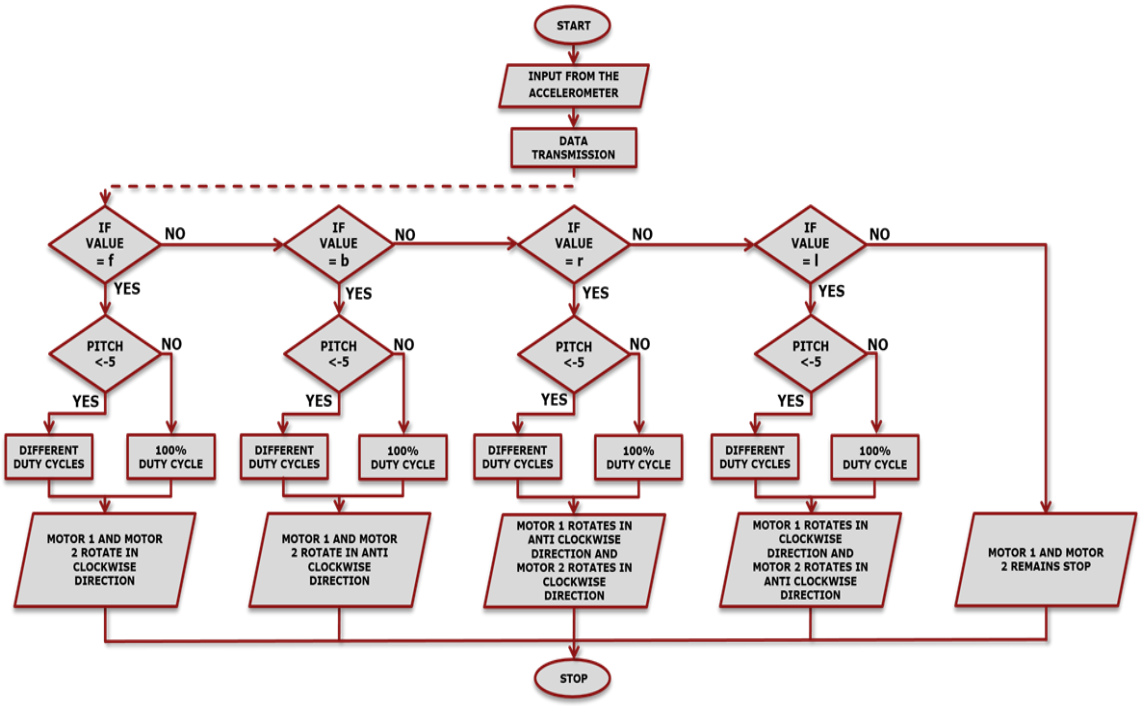

Figure 6. Flowchart of the proposed system

This system is an automated head tilt-movement controlled wheelchair that can work using head movements in any direction, i.e., Forward, backward, right, and left. When the person does not tilt his head in either direction, it stops. In the proposed system shown in Fig. 7, an accelerometer of 3-axis with high resolution (13-bit) measurement at up to ±16 g is interfaced with a microcontroller. The purpose of this Accelerometer is

to measures the static acceleration of gravity in tilt-sensing applications, as well as dynamic acceleration resulting from motion or shock. Whenever the patient tilts its head, this movement is detected by the Accelerometer. In this work, we used an accelerometer (ADXL 335) with an ATmega328 controller. The controller has builtin10-bit ADC (analog to digital converter). A 10-bit ADC has 210 =1,024 possible output codes. Hence, the resolution is 5V/1,024 or 4.88mV; this is called the reference value. But, the values of possible outputs of ADCs come at various speeds and provide differing degrees of accuracy. In our case, the ADC values vary from 0 to 1023. If the accelerometer value of the pitch (y-axis rotation) lies between 500 to 814, the master controller sends the command 'F" to the slave controller, and the wheelchair moves toward the forward direction. Similarly, if the accelerometer value of the pitch (y-axis rotation) reaches between 200 to 401, the master controller sends the command 'B" to the slave controller, and the wheelchair moves toward the backward direction. Likewise, to obtain left and right motion, we have set the accelerometer values of roll (x-axis rotation) between 100 to 300 (for left) and 700 to 100 (for right). The command 'L' and 'R' send by the master controller to the slave when the set roll values arise. It is worth mentioning that the values of ADC are selected after several trials by considering the involuntary movements of the head. High performance, low power Atmel AVR 8-bit microcontroller reads the signals which are generated as a result of head movement and transmits some specific alphabetic data in the form of characters to the slave microcontroller wirelessly through the two-way (full-duplex) Bluetooth modules. As soon as data begins to arrive at the slave controller, the MPU6050 3-axis gyroscope inside, interfaced with the slave microcontroller, starts measuring the orientation angles (pitch) of the wheelchair, as shown in Figure 6. The logic on which the DC geared motors rotate or the polarities of the voltages are totally based on the received alphabetic data characters. The slave microcontroller reads the signals which are generated as a result of the orientation angles of the wheelchair, thus induces pulse width modulation to the H-bridge, which is an electronic circuit used to switch the polarity of a voltage applied to a load. In our system, we could also use the relays instead of using H-bridge, but one of the main objectives of our system is to control or vary the speed of the wheelchair, so this feature is not possible with the relays. On the basis of originated logic and induced duty cycles, the motor will start rotating, which operates the wheelchair in a particular direction at a specific speed.

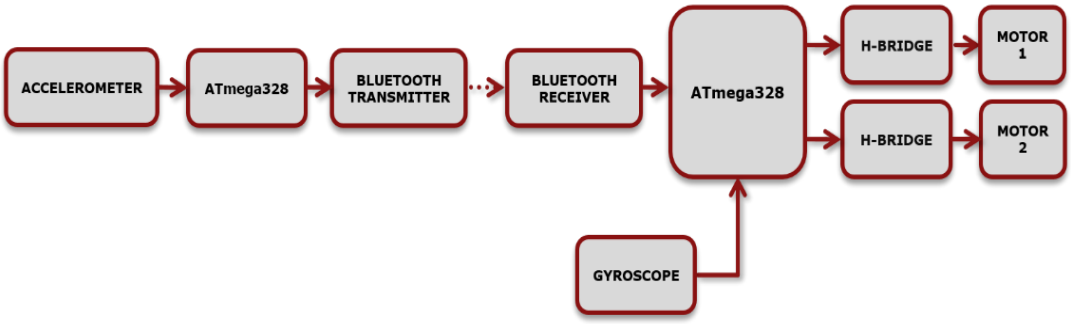

Figure 7. Block diagram of the proposed system

5. METHODOLOGY

The system utilizes two DC geared motors, a helmet circuit, and a wheelchair circuit. The deployed DC geared motors selection is purely based on mathematical calculation. The helmet circuit is comprised of an accelerometer sensor, ATmega328 microcontroller, and Bluetooth module. Wheelchair circuit comprised of Bluetooth module, ATmega328 microcontroller, gyroscope, and power MOSFET. The low-power Bluetooth modules are configured in a master-slave combination to transmit the signal wirelessly. The tiltation of the head is sensed by the Accelerometer, and the microcontroller reads the data from the coordinates of the Accelerometer. On behalf of reading data, the microcontroller generates the signal, which is transmitted by the master Bluetooth module wirelessly from the head circuit to the wheelchair circuit. Through the slave Bluetooth module, the microcontroller receives the signal and controls the directions of the wheelchair as per the head movements of the user with the help of power MOSFETs and DC geared motor. The variation in the speed of the wheelchair on the normal or inclined surface is controlled with the help of a gyroscope that is also deployed in the wheelchair circuit, and its responsibility is to give continuous feedback of the wheelchair's orientation angles to the microcontroller.

Table 2 shows the motor's rotation and wheelchair operating direction. The forward motion achieves when the slave controller gives two positive signals to the motor driver; as a result, both motors rotate clockwise. Similarly, the backward motion achieves when the slave controller gives two negative inputs to the motor driver; as a result, both motors rotate anti-clockwise. Likewise, left and right movements are achieved,

and one motor rotates clockwise, and one motor rotates anti-clockwise when one positive and one negative signal are received by the slave controller. We have also tested our wheelchair while taking a right and left turns by stopping one motor instead of anti-clockwise, but in that case, the wheelchair requires too much space to take turns, and this also increases the load on one motor. In our method, the wheelchair takes turns on its center of axis without consuming the unnecessary space and makes a smooth turn without any resistance or load.

Table 2. The motors rotation and wheelchair direction

DIRECTION	MOTOR 1	MOTOR 2
FORWARD	CLOCKWISE	CLOCKWISE
BACKWARD	ANTI-CLOCKWISE	ANTI-CLOCKWISE
RIGHT	ANTI-CLOCKWISE	CLOCKWISE
LEFT	CLOCKWISE	ANTI-CLOCKWISE

Table 3 reveals the gyroscope orientation angles of a wheelchair on an inclined plane or rough surface and duty cycles of PWM generated by the microcontroller. If the pitch angle is greater than -5° and the roll angle is between -10° to 10°, then the duty cycle would be 100%; as a result, the wheelchair moves at full speed. When the pitch angle is between -5° and -15°, and roll angle is between -10° and 10°, then the controller generates an 80% duty cycle; as a result, the wheelchair starts to decrease its speed. The wheelchair further decreases its speed when the pitch angle is between -15° and -35° and the roll angle is between -10° to 10°. The wheelchair stops, and the duty cycle becomes zero when the pitch angle becomes less than -35°, and the roll angle lies between -10° to 10°. These duty cycles totally depend on the pitch angle of the gyroscope mounted on the wheelchair to monitor its orientation and provide continuous feedback to the microcontroller. The duty cycles decrease with the increase in the inclined plane or sloped surface.

Table 3. Orientation angles of wheelchair and duty cycle of PWM

ANGLES	DUTY CYCLE
if(Pitch > -5 && Roll > -10 && Roll < 10)	100%
if(Pitch < -5 && Pitch > -15 && Roll > -10 && Roll < 10)	80%
if(Pitch < -15 && Pitch > -25 && Roll > -10 && Roll < 10)	60%
if(Pitch < -25 && Pitch > -35 && Roll > -10 && Roll < 10)	40%
if(Pitch < -35 && Roll > -10 && Roll < 10)	0%

6. EXPERIMENTAL RESULTS

After the research, design, and implementation of our proposed smart robotic wheelchair, we have tested and analyzed its response for different situations such as normal, rough, and inclined surfaces; the wheelchair is operating entirely and efficiently for all the conditions. Results are indeed the same as desired, and almost 99% accuracy has been achieved. Moreover, the tiny circuit mounted inside the cap with Accelerometer and the circuit mounted on the wheelchair with a gyroscope work precisely and effectively on account of the head's gestures. Using head commands, we can easily and smoothly drive the wheelchair in the forward direction, backward, left, and right direction, furthermore, on the inclined plane and stop the wheelchair when the user wishes.

(a) Forward direction (b) Backward direction (c) Right direction (d) Left direction

Figure 8. Movement of the wheelchair on normal or plane surface

Figure 8 shows the movements of the wheelchair in the forward, backward, right, and left direction as per the user's head tiltation.

(a) Downward movement. (b) Upward movement.

Figure 9. Movement of the wheelchair on the slope or inclined surface

Figure 9 shows the testing of the wheelchair on the inclined plane or slope. In these figures, the wheelchair smoothly moves downward and upward on the inclined plane without any type of slip or free movement.

7. SIMULATION RESPONSES

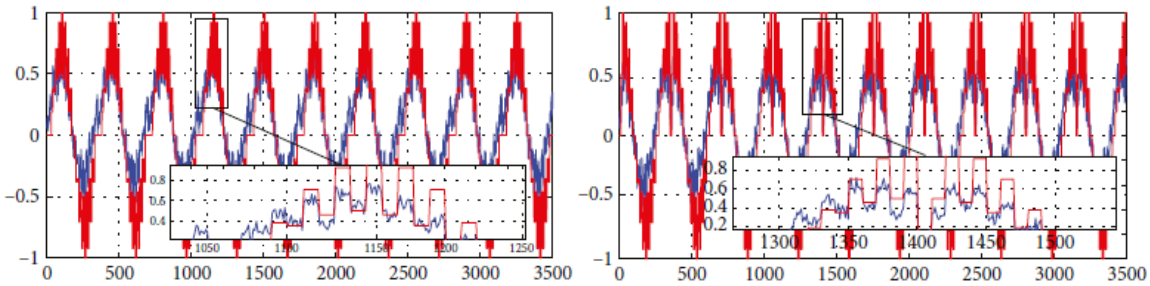

(a) Forward direction response (b) Backward direction response

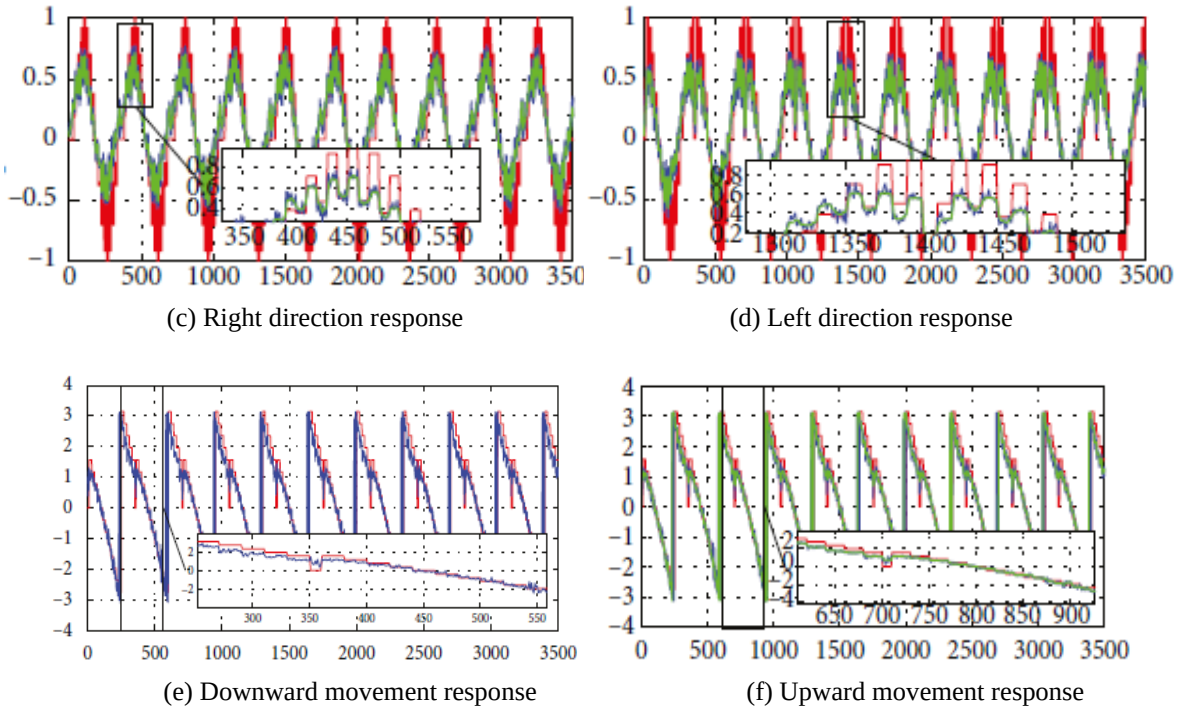

(c) Right direction response (d) Left direction response

(e) Downward movement response (f) Upward movement response

Figure 10. Simulation results of the wheelchair movement

The simulation tests the validity of the proposed approach compared with previously proposed models and parameter adjustments. These results are obtained via employing the Kalman filter on our sensor results. Figures 10(a) and (b) are the graphs between the time (x-axis) and the pitch angle (y-axis). Here, the blue signals correspond to the actual results of pitch up and pitch down angles of an accelerometer with respect to time that refers to the upward and downward motions of the developed wheelchair; however, the red signals correspond to the filtered and smooth output. Similarly, in Figure 10 (c) and (d), the graphs show the actual accelerometer sensor and filtered output with respect to time. The green signals correspond to the actual sensor results, and red signals refer to the filtered results which are plotted between roll angles(y-axis) and time (x-axis). Likewise, Figures (e) and (f) exhibits the gyroscope yaw angles (y-axis) actual and filtered results with respect to time, which correspond to the inclined plane movement of the wheelchair. The simulation concentrated on the scenes where the user goes straight up and down on an inclined plane and turns on the head's instructions. From these filtered results, we proved that the proposed method could eliminate the moving distance and increase lateral force without losing the pitch angle stability. It can also be said that through this simulation, the validity of the proposal has been validated.

8. CONCLUSION AND PERSPECTIVES

Our proposed system is not the only novel in designing, but also it has conquered all the drawbacks and issues found in previously designed wheelchairs. With the finalization and execution of our system, we have concluded that our proposed system is ideal for the handicapped, paralyzed, disabled, quadriplegic, and for those people who are suffering from spinal cord injuries. Furthermore, it is a very efficient, user-friendly, and cost-effective system in comparison with the previously proposed systems.

REFERENCES

[1] Yassine Rabhi, Makrem Mrabet, Farhat Fnaiech, "Intelligent Control Wheelchair Using a New Visual Joystick", Journal of Healthcare Engineering, vol. 2018, Article ID 6083565, 20 pages, 2018. https://doi.org/10.1155/2018/6083565.

[2] Gupta, Abhishek & Joshi, Neeraj & Chaturvedi, Nikhil & Sharma, Sonam & Pandar, Vikash. (2016). Wheelchair Control by Head Motion Using Accelerometer. International Journal of Electrical and Electronics Research. 4. 2348-6988.

[3] S. Hamatani, T. Nozaki and T. Murakami, "Steering control in multi-degrees-of-freedom two-wheeled wheel chair on slope environment," IECON 2016 - 42nd Annual Conference of the IEEE Industrial Electronics Society, Florence, 2016, pp. 6181-6186, doi: 10.1109/IECON.2016.7793397.

[4] S. Nasif and M. A. G. Khan, "Wireless head gesture controlled wheel chair for disable persons," 2017 IEEE Region 10 Humanitarian Technology Conference (R10-HTC), Dhaka, 2017, pp. 156-161, doi: 10.1109/R10-HTC.2017.8288928.

[5] U. Mohammad and M. Anas, "Design of a low cost DIY moving wheel chair using ATmega1284P based on retina movement for the persons disabled with quadriplegia," 2015 Annual IEEE India Conference (INDICON), New Delhi, 2015, pp. 1-4, doi: 10.1109/INDICON.2015.7443544.
[6] Purwanto D, Mardiyanto R, Arai K. Electric wheelchair control with gaze direction and eye blinking. Artificial Life and Robotics. 2009 Dec;14(3):397-400.
[7] Francis WC, Umayal C, Kanimozhi G. Brain-Computer Interfacing for Wheelchair Control by Detecting Voluntary Eye Blinks. Indonesian Journal of Electrical Engineering and Informatics (IJEEI). 2021 May 31;9(2):521-37.
[8] Królak A, Strumiłło P. Eye-blink detection system for human-computer interaction. Universal Access in the Information Society. 2012 Nov;11(4):409-19.
[9] Nakanishi M, Mitsukura Y. Wheelchair control system by using electrooculogram signal processing. InThe 19th Korea-Japan Joint Workshop on Frontiers of Computer Vision 2013 Jan (pp. 137-142). IEEE.
[10] Riyadi MA, Prakoso T, Whaillan FO, Wahono MD, Hidayatno A. Classification of EEG-based brain waves for motor imagery using support vector machine. In2019 International Conference on Electrical Engineering and Computer Science (ICECOS) 2019 Oct 2 (pp. 422-425). IEEE.
[11] R. Akmeliawati, F. S. B. Tis and U. J. Wani, "Design and development of a hand-glove controlled wheel chair," 2011 4th International Conference on Mechatronics (ICOM), Kuala Lumpur, 2011, pp. 1-5, doi: 10.1109/ICOM.2011.5937126.
[12] Lontis ER, Bentsen B, Gaihede M, Struijk LN. Wheelchair control with the tip of the tongue. InReplace, Repair, Restore, Relieve–Bridging Clinical and Engineering Solutions in Neurorehabilitation 2014 (pp. 521-527). Springer, Cham.
[13] M. A. Rahman Apu, I. Fahad, S. A. Fattah and C. Shahnaz, "Eye Blink Controlled Low Cost Smart Wheel Chair Aiding Disabled People," 2019 IEEE R10 Humanitarian Technology Conference (R10-HTC)(47129), Depok, West Java, Indonesia, 2019, pp. 99-103, doi: 10.1109/R10-HTC47129.2019.9042446.
[14] Xu, Cun Shan. "Application Research of MEMS ADXL345." Advanced Materials Research, vol. 457–458, Trans Tech Publications, Ltd., Jan. 2012, pp. 1550–1553. Crossref, doi:10.4028/www.scientific.net/amr.457-458.1550.
[15] Aarai, Kohei & Mardiyanto, Ronny. (2011). A Prototype of Electric Wheelchair Controlled by Eye-Only for Paralyzed User. Journal of Robotics and Mechatronics. 23. 10.20965/jrm.2011.p0066.
[16] Taha, Zahraa. (2017). Wireless Communication for Gas Detection using 433RF Modules and Arduino Processor. 975-8887.
[17] Toudjeu, Ignace & Hamam, Yskandar & Djouani, Karim & Van Wyk, Barend & Monacelli, Eric. (2012). Modelling and Simulation of a User-Wheelchair-Environment System. 10.2316/P.2012.761-022.
[18] S. Oh and Y. Hori, "Development of an Extended Operational Kalman of Power Assist Wheelchair," 2006 IEEE International Conference on Industrial Technology, 2006, pp. 358-363, doi: 10.1109/ICIT.2006.372377.
[19] B. W. Johnson and J. H. Aylor, "Dynamic Modeling of an Electric Wheelchair," in IEEE Transactions on Industry Applications, vol. IA-21, no. 5, pp. 1284-1293, Sept. 1985, doi: 10.1109/TIA.1985.349556.
[20] S. O. Onyango, Y. Hamam, M. Dabo, K. Djouani and G. Qi, Dynamic Control of an Electrical Wheelchair on an Incline, Proc. IEEE AFRICON '09, Nairobi, Kenya, 23-25 Sept. 2009, pp. 1-6.